

Topological comparison between the stochastic and the nearest-neighbour declustering methods through network analysis

Antonella Peresan¹, Elisa Varini², and Jiancang Zhuang³

¹National Institute of Oceanography and Experimental Geophysics

²Istituto di Matematica Applicata e Tecnologie Informatiche

³Institute of Statistical Mathematics

November 26, 2022

Abstract

Earthquake clustering is a relevant feature of seismic catalogs, both in time and space. Several methodologies for earthquake cluster identification have been proposed in the literature in order to characterise clustering properties and to analyse background seismicity. We consider two recent data-driven declustering techniques, one is based on nearest-neighbor distance and the other on a stochastic point process. These two methods use different underlying assumptions and lead to different classifications of earthquakes into background events and secondary events. We investigated the classification similarities by exploiting graph representations of earthquake clusters and tools from network analysis. We found that the two declustering algorithms produce similar partitions of the earthquake catalog into background events and earthquake clusters, but they may differ in the identified topological structure of the clusters. Especially the clusters obtained from the stochastic method have a deeper complexity than the clusters from the nearest-neighbor method. All of these similarities and differences can be robustly recognised and quantified by the outdegree centrality and closeness centrality measures from network analysis.

1 **Topological comparison between the stochastic and the**
2 **nearest-neighbour declustering methods through**
3 **network analysis**

4 **E. Varini¹, A. Peresan², and J. Zhuang³**

5 ¹C.N.R. - Institute of Applied Mathematics and Information Technology
6 via Bassini 15, 20133 Milano, Italy

7 ²National Institute of Oceanography and Experimental Geophysics

8 CRS-OGS, via Treviso 55, 33100 Udine, Italy

9 ³Institute of Statistical Mathematics, Research Organization of Information and Systems
10 10-3 Midori-Cho, Tachikawa, Tokyo 190-8562, Japan

11 **Key Points:**

- 12 • Two recent data-driven declustering methods are compared, one based on nearest-
13 neighbor distance and one on the ETAS model
- 14 • Similarities in classification and in earthquake clusters are investigated by tree graphs
15 and tools from network analysis
- 16 • Obtained clusters are consistent, though nearest-neighbor method usually provides
17 simpler structures than stochastic declustering method

Corresponding author: Antonella Peresan, aperesan@inogs.it

Abstract

Earthquake clustering is a relevant feature of seismic catalogs, both in time and space. Several methodologies for earthquake cluster identification have been proposed in the literature in order to characterize clustering properties and to analyze background seismicity. We consider two recent data-driven declustering techniques, one is based on nearest-neighbor distance and the other on a stochastic point process. These two methods use different underlying assumptions and lead to different classifications of earthquakes into background events and secondary events. We investigated the classification similarities by exploiting graph representations of earthquake clusters and tools from network analysis. We found that the two declustering algorithms produce similar partitions of the earthquake catalog into background events and earthquake clusters, but they may differ in the identified topological structure of the clusters. Especially the clusters obtained from the stochastic method have a deeper complexity than the clusters from the nearest-neighbor method. All of these similarities and differences can be robustly recognized and quantified by the outdegree centrality and closeness centrality measures from network analysis.

Plain Language Summary

Clustering, in both space and time, is a widely recognised feature of seismicity. An adequate identification of earthquake clusters allows splitting seismicity into background and clustered events (e.g. aftershocks), and is an essential step in several studies, ranging from seismic hazard assessment to long- and short-term earthquake forecasting. Also, the space-time patterns of identified clusters may provide useful insights on the structural and dynamic tectonic features of a region. Among the several methods proposed so far to identify and characterise seismic clusters, we consider two recent data-driven declustering techniques, one based on nearest-neighbor distance and the other on a stochastic point process. These two methods use different underlying assumptions and may lead to different classifications of earthquakes into background events and clustered events. Therefore this study aims to compare their performances, including clusters structure characterisation, by exploiting tree graph representations and tools from network analysis. We found that: (1) the two declustering algorithms produce similar partitions of the earthquake catalog; (2) they may differ in the internal structure outlined for individual clusters, with the nearest-neighbor method usually providing simpler structures than stochastic declustering method; and (3) these features can be robustly quantified by centrality measures widely used in network analysis.

1 Introduction

Short-term earthquake clustering is a widely recognised feature of seismic activity, which eventually complicates the analysis of seismicity, especially when we evaluate long-term earthquake risks. An ideal partition of an earthquake catalog is into two subsets of events, referred as background seismicity and secondary seismicity, respectively. Background events are intended as spontaneous or independent earthquakes; secondary events are considered as triggered by other earthquakes, therefore manifestly dependent events, generally forming spatio-temporal clusters and producing a significant increase of the seismicity rate. It is often supposed that background events are representative of the long-term spatio-temporal behaviour of seismicity in a region. Poisson model, renewal model, and stress release model are typically assumed as suitable stochastic processes to describe background events (Vere-Jones, 1978; Rotondi, 2010; Rotondi & Varini, 2019). On the other hand, the identification of earthquake clusters is important to understand and to forecast the spatio-temporal evolution of a seismic sequence on short time scales; the Omori-Utsu formula, the Epidemic-Type Aftershock-Sequence model and its exten-

67 sions are typically used to model earthquake clusters, such as swarms or aftershock se-
68 quences (Ogata, 1998).

69 However, an objective and commonly agreed method for separating earthquake clus-
70 ters from each other and from the background seismicity is critical. There are several
71 declustering algorithms in the literature (van Stiphout et al. (2012) and references therein),
72 which are likely to identify different earthquake clusters and, accordingly, different declus-
73 tered versions of a catalog.

74 The most used declustering algorithms are the mainshock-window method by Gardner
75 and Knopoff (1974) and the linked-window method by Reasenber (1985), due to their
76 simplicity and software availability: the former removes all earthquakes in a certain space-
77 time window around each suitably defined mainshock; the latter performs scans within
78 certain space-time windows of each event in the catalog in order to form clusters of events
79 and then replace each cluster with a single event (e.g. the first, or the larger). The draw-
80 back of window methods is that they require some subjective choices, such as the def-
81 inition of mainshock or the dimensions of the space-time windows, which might seriously
82 influence the results.

83 Among the valid alternatives to window-based methods, we focus on two recently
84 proposed declustering algorithms: the nearest-neighbor method by Zaliapin and Ben-
85 Zion (2013, 2016) and the stochastic declustering method by Zhuang et al. (2002, 2004)
86 and Zhuang (2006). They have been the subject of several recent papers to which the
87 readers can refer for additional details (e.g. Peresan and Gentili (2018), Zhang and Shearer
88 (2016), Nandan et al. (2019) for the nearest-neighbor method and Davoudi et al. (2018),
89 Zhuang et al. (2005), Talbi et al. (2013) for the stochastic declustering method). Both
90 methods are data-driven and can be satisfactorily applied to decompose the seismic cat-
91 alog into background seismicity and sequences of clustered earthquakes.

92 In addition, both methods allow studying the internal structure of the identified
93 sequences (or several probable realizations of it, in the case of stochastic declustering method)
94 since they provide the connections between events forming each cluster.

95 For example Wang et al. (2010) compared the Reasenber's, Kagan's, and Zhuang's
96 methods; Talbi et al. (2013) dealt with the methods of Gardner and Knopoff, Reasen-
97 berg, and stochastic declustering. However, in-depth comparison was carried out so far
98 between these more recent methods.

99 This study focuses on the nearest-neighbor and the stochastic declustering algo-
100 rithms because they can be used not only to identify background seismicity, but also to
101 investigate the properties and internal structure of seismic clusters (Zhuang et al., 2004;
102 Guo et al., 2015, 2017). The aim is to compare the features of clusters identified by the
103 two algorithms exploiting tools and measurements from network analysis. Moreover the
104 research aims to improve our understanding of the role of moderate earthquakes in the
105 region, providing in the meanwhile a characterization of seismicity patterns and their vari-
106 ations at short-term space-time scales.

107 This article is organised as follows: a short description of both declustering meth-
108 ods is given in Section 2; the seismicity of Northeastern Italy and the related earthquake
109 data sets, to be used as a case study, are introduced in Section 3. Section 4 gives the com-
110 putational details to fit the declustering algorithms to the data and then it provides a
111 global comparison of the background seismicity and earthquakes clusters obtained from
112 the two methods. Section 5 deals with the analysis of the clusters structure by exploit-
113 ing graphical tools and quantitative methods from network theory. Conclusions are drawn
114 in Section 6.

2 Declustering Algorithms Under Examination

Given a catalog $\{(t_i, x_i, y_i, m_i) : i = 1, \dots, n\}$, where n is the total number of earthquakes, and t_i , (x_i, y_i) , and m_i are the occurrence time, epicentral location, and magnitude, respectively, the numerical algorithms of these two declustering methods are given in following subsections.

2.1 Nearest-neighbor algorithm (NN)

This approach is based on the NN-distance (nearest-neighbor distance) between two earthquakes in the space-time-energy domain, as defined by Baiesi and Paczuski (2004):

$$\eta_{ij} = (t_j - t_i) r_{ij}^{d_f} 10^{-bm_i} \quad (1)$$

where $t_i < t_j$ and r_{ij} is the spatial distance between events i and j . This metric exploits the following statistical properties of seismicity to quantify the correlation between earthquakes: the inter-occurrence time, the fractal dimension of the hypocentres distribution, and the Gutenberg–Richter law. There are only two unknown parameters, namely fractal dimension d_f and b -value, which are jointly and robustly estimated by the Unified Scaling Law for Earthquakes (USLE) method (Nekrasova et al., 2011); a separation distance η_0 is also estimated in order to identify clusters of events (details in Peresan and Gentili (2018)).

The nearest-neighbor distance η_{ij} can be equivalently decomposed into the corresponding rescaled space (R_{ij}) and rescaled time (T_{ij}) distances from the parent to its offspring event (Zaliapin et al., 2008), namely $\eta_{ij} = T_{ij} R_{ij}$, where: $T_{ij} = t_j 10^{-bm_i/2}$ and $R_{ij} = r_{ij}^{d_f} 10^{-bm_i/2}$.

Accordingly each event j is connected to its nearest-neighbor $i = \arg \min_{k:k < j} \eta_{kj}$. Then, by removing all connections η_{ij} such that $\eta_{ij} > \eta_0$, the earthquake catalog is unambiguously partitioned on distinct clusters, each containing at least one event (Zaliapin & Ben-Zion, 2013, 2016). The maximum magnitude event of each cluster is labelled as background event and the remaining events of the clusters are included in the secondary seismicity.

2.2 Stochastic declustering algorithm (SD)

This approach is based on the space-time ETAS (epidemic-type aftershock sequence) model (Ogata, 1998), a branching point process defined by its intensity function conditional on the observation history \mathcal{H}_t :

$$\lambda(t, x, y | \mathcal{H}_t) = \mu(x, y) + \sum_{k:t_k < t} g(t - t_k, x - x_k, y - y_k; m_k) \quad (2)$$

where $\mu(x, y)$ is the spatial background rate of a time-homogeneous Poisson process and, at time t , $g(t - t_k, x - x_k, y - y_k; m_k)$ is the contribution to seismic hazard due to triggering effects of the k -th earthquake. The explicit functional forms in Eq. (1) are the following:

$$\begin{aligned} \mu(x, y) &= \nu \cdot u(x, y) \\ g(t, x, y; m) &= A e^{\alpha(m-m_0)} \cdot (p-1) e^{p-1} (t+c)^{-p} \cdot \\ &\quad \cdot \frac{1}{2\pi d e^{\alpha(m-m_0)}} \exp \left\{ -\frac{1}{2} \frac{x^2 + y^2}{d e^{\alpha(m-m_0)}} \right\} \end{aligned} \quad (3)$$

where $\nu, A, c, \alpha, p, d, q, \gamma$ are positive parameters and $u(x, y)$ is an unknown spatial function (Zhuang et al., 2002). An iterative algorithm simultaneously provides the maximum likelihood estimates of the eight model parameters and a non parametric kernel estimate of the spatial background rate.

158 According to point process theory, the probability that event j is generated by the
 159 background process is $\varphi_j = \mu(x_j, y_j)/\lambda(t_j, x_j, y_j | \mathcal{H}_{t_j})$, and the probability that it is
 160 triggered from previous event i is $\rho_{ij} = g(t_j - t_i, x_j - x_i, y_j - y_i; m_i)/\lambda(t_j, x_j, y_j | \mathcal{H}_{t_j})$.
 161 Thinning (sampling) the process according to these probabilities allows splitting the cat-
 162 alog into background events and triggered events, and also setting connections between
 163 triggering and triggered events (Zhuang et al., 2002, 2004; Zhuang, 2006). The first event
 164 of each cluster is labelled as background event, which may not be the maximum mag-
 165 nitude event within the cluster; it is named ancestor because it represent the earthquake
 166 that triggers others in the cluster. The remaining events of the clusters are included in
 167 the secondary seismicity and are called descendants. Unlike NN method, SD algorithm
 168 can provide many declustered catalogs by simulation.

169 2.3 Differences and connections between the NN and SD methods

170 Notably the two methods have a different definition of background events: while
 171 NN assigns to the background seismicity the largest event from each cluster (i.e. the main-
 172 shock), SD assigns to it the first event of the cluster (not necessarily the mainshock); there-
 173 fore the declustered catalogs may differ, particularly when foreshocks are identified.

174 The NN declustering method has some connections with the stochastic decluster-
 175 ing method. Firstly, the NN-distance η_{ij} takes a similar form as $1/g(t_j - t_i, x_j - x_i, y_j -$
 176 $y_i; m_i)$. If we consider an ETAS-like model with the conditional intensity

$$177 \lambda_0(t, x, y | \mathcal{H}_t) = \mu_0 + A \sum_{i:t_i < t} (t - t_i)^{-1} r(x_i, y_i; x, y)^{-d_f} 10^{bm_i}, \quad (4)$$

178 where $r(x, y; x', y')$ is the Euclidean distance between (x, y) and (x', y') , the quantity $\rho_{ij}^{(0)} =$
 179 $A(t_j - t_i)^{-1} r(x_i, y_i; x_j, y_j)^{-d_f} 10^{bm_i} / \lambda_0(t_j, x_j, y_j | \mathcal{H}_{t_j})$ is proportional to the recipro-
 180 cal of η_{ij} . In this new model the background rate μ_0 is an unknown constant and A is
 181 also unknown, which are in fact connected to the NN method through $\eta_0 = A/\mu_0$.

182 The basic differences between these two methods are clear.

- 183 1. The NN method classifies the clusters based on the minimum distance η_{ij} , which
 184 corresponds, for each event, to the largest probability ρ_{ij} , among the probabili-
 185 ties that the event is from background seismicity or triggered by one of the pre-
 186 vious events, according to the model in (4). The SD method, on the other side,
 187 makes use of the full probability distribution of ρ_{ij} , leading to several possible clus-
 188 ter classifications. As a rule, a probabilistic-manner resampling is recommended
 189 to reflect the uncertainty in the classification of the family tree; however, SD can
 190 also classify the clusters based on the maximum probability ρ_{ij} , in the same man-
 191 ner as the NN method.
- 192 2. The NN method implicitly estimates the classification parameter η_0 , approximately
 193 according to the separation between two modes of the NN-distance distribution;
 194 the two remaining parameters, namely the b-value and the fractal dimension of
 195 epicenters, are estimated independently, and used as a priori input information.
 196 No explicit assumption is made about the background seismicity, which can be in-
 197 homogeneous in space (Zaliapin et al., 2008) and possibly also in time. The SD
 198 method is based on the ETAS model, where the model parameters and the op-
 199 timal non-homogeneous background rate are estimated through MLE procedure,
 200 thus providing a summary description of the considered data set. Accordingly, the
 201 NN method allows for a rather fast and robust identification of clusters, with less
 202 stringent requirements about the catalog completeness and homogeneity, while the
 203 SD provides a more detailed, specific and sophisticated data description and clas-
 204 sification, requiring high-quality catalogs.

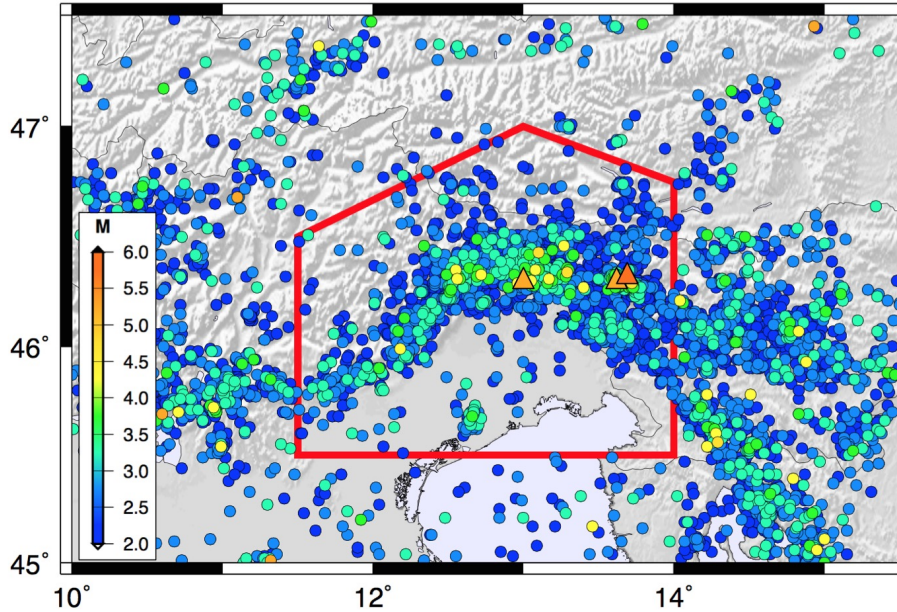


Figure 1. The study region (red polygon) and the epicentres of the earthquakes occurred since 1977. The strongest earthquakes, with magnitude larger than 5.0, are marked by triangles.

3 Study Region and Data

The study region, which comprises North-Eastern Italy and Western Slovenia, is located along the northern edge of Adria micro-plate, at the transition between Alpine and Dinaric fault systems. Earthquakes are mostly shallow (up to 12 km), and are prevalently of thrust type to the west and strike-slip to the east. The instrumental seismicity recorded during about 40 years, prevalently consists of low to moderate earthquakes, only occasionally exceeding magnitude 4.0; the largest earthquake was recorded in 1998 (M 5.6), nearby the border between Italy and Slovenia. Despite the moderate seismic activity that has recently affected this region, the historical seismicity testifies to its high seismic hazard and high vulnerability. According to the Italian Parametric Earthquake Catalogue CPTI15 (Rovida et al., 2014), at least six destructive earthquakes with magnitude larger than 6.0 hit that area in the past millennium, the most recent one being the M 6.4 1976 Friuli earthquake (Slejko et al., 1999).

To investigate the clustering features in the study region, we consider the earthquake bulletins compiled at the National Institute of Oceanography and Experimental Geophysics, which include 27353 earthquakes occurred in the time span from 7 May 1977 to 30 April 2018, and with duration magnitude up to M_d 5.6. Fig. 1 shows the distribution of earthquake epicentres, as well as the study region, which is a polygonal area delimited by the following five vertices: (11.5, 45.5); (11.5, 46.5); (13.0, 47.0); (14.0, 46.75); (14.0, 45.5). A detailed analysis of the data completeness in space and time, including delineation of the study region and estimation of the scaling parameters of seismicity, was carried out by Peresan and Gentili (2018). Within the identified area (red polygon in Fig. 1), the bulletins can be considered fairly complete for magnitudes $M \geq 2.0$ during the whole time span 1977-2018 (Fig. 2), except for a time interval between December 1990 and May 1991, when data acquisition was interrupted due to a fire accident (Fig. 3, bottom panel).

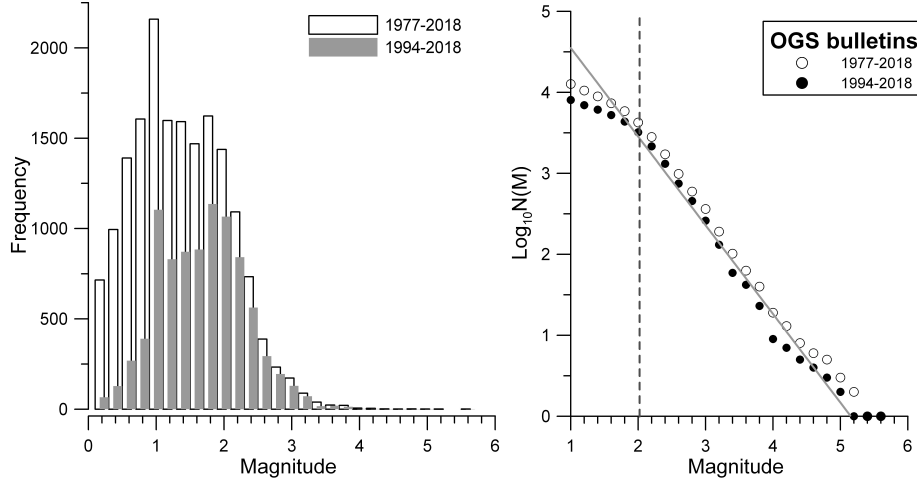


Figure 2. Histogram on magnitude (left) and estimated Gutenberg–Richter law (right) for the full (1977-2018) and the complete (1994-2018) data sets.

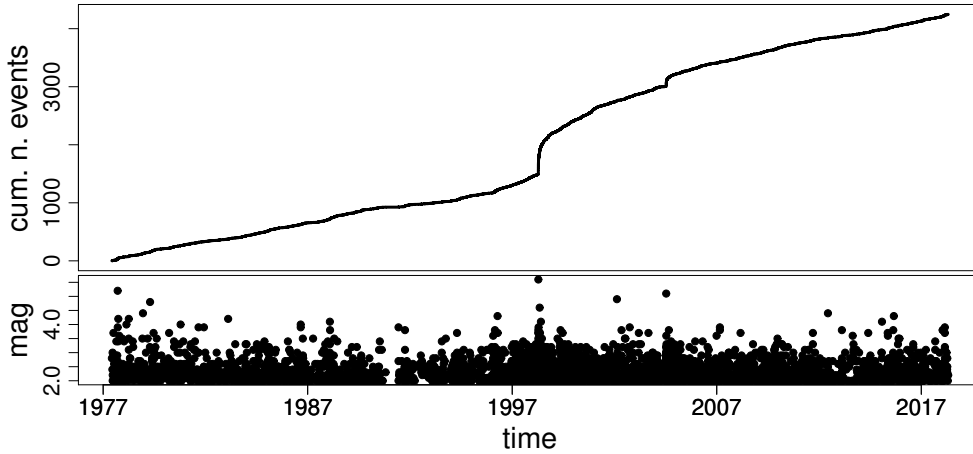


Figure 3. Full data set (1977-2018, $M \geq 2.0$): cumulative number of events versus time (top) and magnitude versus time (bottom).

231 Since the data are certainly incomplete in the early 1990s, two subsets of the cat-
 232 alog are considered hereinafter. The former, referred to as the complete data set, includes
 233 all the 3219 earthquakes having magnitude at least 2.0 and occurred since 1994; the sta-
 234 tistical completeness and the b-value of the Gutenberg-Richter law have been estimated
 235 using only this part of the data (Fig. 2). The latter subset, named the full data set, is
 236 obtained from the catalog by setting a minimum threshold magnitude equal to 2.0; there-
 237 fore, it covers the entire time span from 1977 to 2018 and it includes 4247 earthquakes
 238 (Fig. 3).

239 4 Declustering Outputs

240 4.1 Declustering settings and global features of the two declustered cat- 241 alogs

242 Both NN and SD algorithms are applied in order to obtain declustered versions of
 243 the full data set.

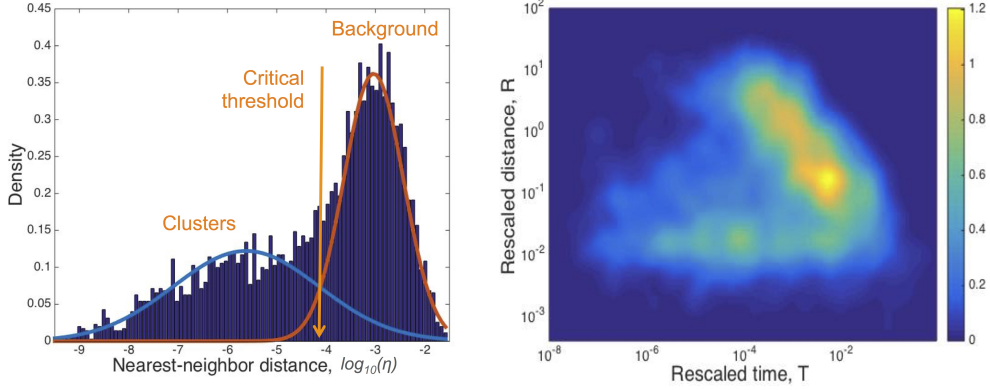


Figure 4. Distributions of NN-distances, between each event and its nearest neighbour, estimated for earthquakes with $M \geq 2.0$ in 1977-2018. Left column: 1D density distribution of $\log \eta$, with estimated Gaussian densities for clustered (blue) and background (red) components. Right column: 2D joint distribution of rescaled space and time distances (R,T).

244 The scaling parameters of NN-algorithm are simultaneously estimated by the USLE
 245 method and their values are $b = 0.9$ and $d_f = 1.1$ as defined in Peresan and Gentili
 246 (2018); the logarithm of the separation distance is automatically set equal to $\log \eta_0 =$
 247 -4.1 (Fig. 4).

248 Based on these parameters, the NN-algorithm delivers its partition of the data set,
 249 which is hereinafter referred to as the NN-catalog. The background seismicity turns out
 250 to be composed by the isolated events (singles) and the largest event of each cluster (i.e.
 251 the mainshocks, the number of which equals the number of clusters); all other events be-
 252 long to the secondary seismicity. Table 1 (top) summarizes the NN-catalog by provid-
 253 ing the number of events assigned to background seismicity and to secondary seismic-
 254 ity, as well as the number of isolated events (singles), the number of identified earthquake
 255 clusters, and the total number of events that temporally precede/follow the strongest earth-
 256 quake that occurred in their own cluster (here conventionally referred to as foreshocks
 257 and aftershocks).

258 As for the SD-algorithm, the complete data set (which ranges from 1994 to 2018)
 259 has been used for the maximum likelihood estimation of ETAS parameters, by assum-
 260 ing that the past history \mathcal{H}_t of the process is given by the full data set (which ranges from
 261 1977 to 2018). The following estimates of the ETAS parameters are thus given: $\nu = 0.6772$,
 262 $A = 0.6656$, $c = 0.0146$, $\alpha = 1.5407$, $p = 1.0378$, $d = 0.00007$, $q = 2.2527$, and
 263 $\gamma = 0.6239$.

264 Fig. 5 shows the estimated total rate $\hat{\lambda}(t, x, y | \mathcal{H}_t)$ in the region, the ratio between
 265 estimated cluster rate and total rate, and the histogram of the estimated background prob-
 266 abilities $\hat{\varphi}_j$ of each event j in the catalog ($j = 1, \dots, n$). According to the SD-method,
 267 several declustered catalogs can be obtained by simulating the connections between events
 268 based on both the estimated background probabilities $\{\hat{\varphi}_j : j = 1, \dots, n\}$ and the es-
 269 timated triggering probabilities $\{\hat{\rho}_{ij} : i, j = 1, \dots, n, i < j\}$. To make the comparison
 270 between the two declustering methods feasible, we decided to select only one of those
 271 simulated catalogs. A reasonable choice is to select the “most probable declustered cat-
 272 alog”, which is obtained by retaining the most probable connections between any pair
 273 of events according to the estimated background and triggering probabilities; the result-
 274 ing partition of the full data set is hereinafter referred to as the SD-catalog. Table 1 (bot-

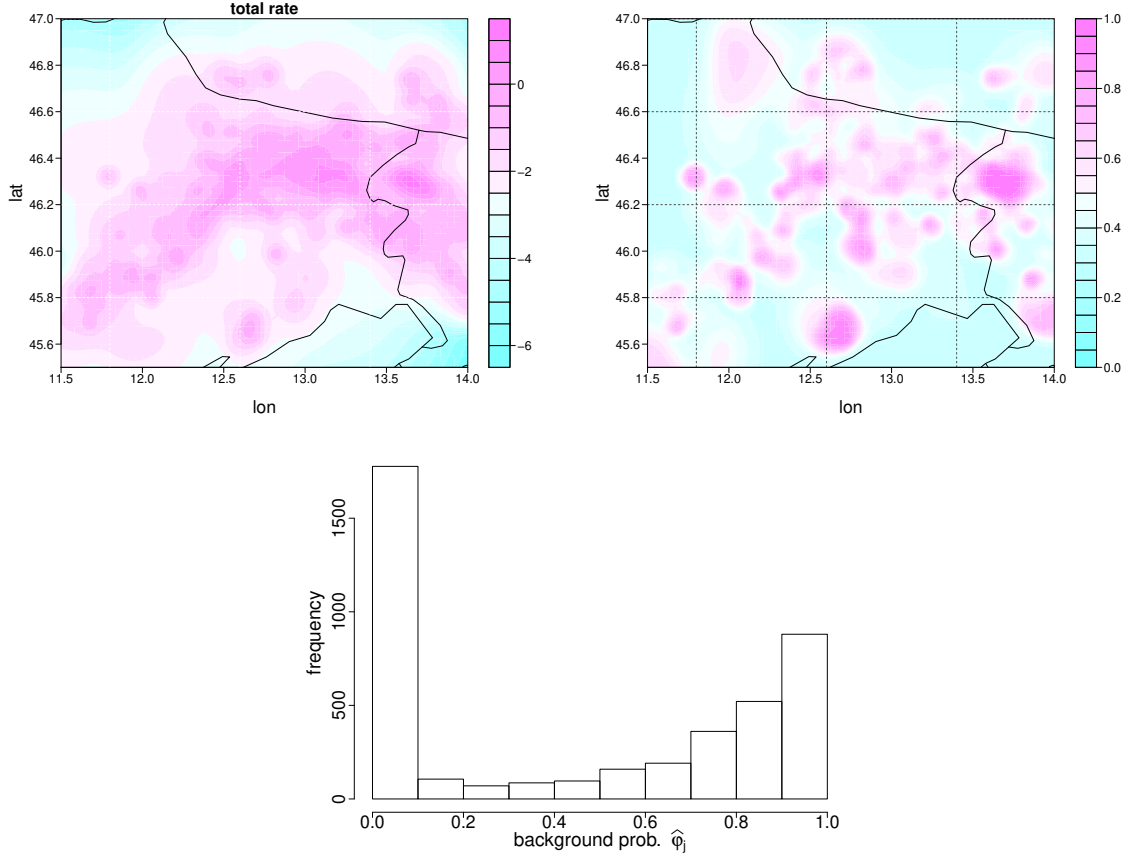


Figure 5. Some results from the SD-algorithm: map of the estimated logarithm of the total rate (top left), map of the ratio between estimated cluster rate and total rate (top right), histogram of the estimated background probabilities for each earthquake in the data set (bottom).

275 tom) summarizes some counts on the SD-catalog, which turn out fairly consistent with
 276 those obtained from NN-method (top of Table 1).

277 4.2 Comparison of clusters size

278 The clusters identified by the NN and SD methods are first of all compared in terms
 279 of cluster size (i.e. number of events composing the cluster), by assuming clusters are
 280 formed by at least two events. The cluster size distributions of NN-catalog and SD-catalog
 281 are shown in Fig. 6; in both cases about 95% of the clusters are composed by less than
 282 10 events and about 85% of the identified clusters has even less than 5 events. This means
 283 that, for both methods, the number of relevant clusters is quite limited, less than 15%
 284 of identified clusters.

285 It is not obvious to establish a one-to-one correspondence between NN-clusters and
 286 SD-clusters, because events from one NN cluster may be separated into different SD clus-
 287 ters. To facilitate the comparison of individual clusters identified by the two decluster-
 288 ing methods, we consider the largest earthquake in each cluster as the representative event
 289 of the cluster. If a NN-cluster and a SD-cluster have the same representative event, we

Table 1. Summaries of the NN-catalog (top) and the SD-catalog (bottom). Tables report the number of events classified as background/secondary seismicity, the number of single events, the number of clusters, the total number of secondary events that occur before/after the maximum magnitude event in their own cluster (foreshock/aftershock). Percentages with respect to the total number of data are also reported.

| NN-catalog | | | | |
|--------------------------------------|----------------------------------|---------------------------------------|------------------------------------|--------------------------------|
| <i>n.background</i> 2468 (58.11%) | | <i>n.secondary</i> 1779 (41.89%) | | <i>n.events</i> 4247 (100%) |
| <i>n.singles</i> 2123 (49.99%) | <i>n.clusters</i> 345 (8.12%) | <i>n.aftershocks</i> 1548 (36.45%) | <i>n.foreshocks</i> 231 (5.44%) | |

| SD-catalog | | | | |
|--------------------------------------|----------------------------------|---------------------------------------|------------------------------------|--------------------------------|
| <i>n.background</i> 2255 (53.10%) | | <i>n.secondary</i> 1992 (46.90%) | | <i>n.events</i> 4247 (100%) |
| <i>n.singles</i> 1884 (44.36%) | <i>n.clusters</i> 371 (8.74%) | <i>n.aftershocks</i> 1685 (39.67%) | <i>n.foreshocks</i> 307 (7.23%) | |

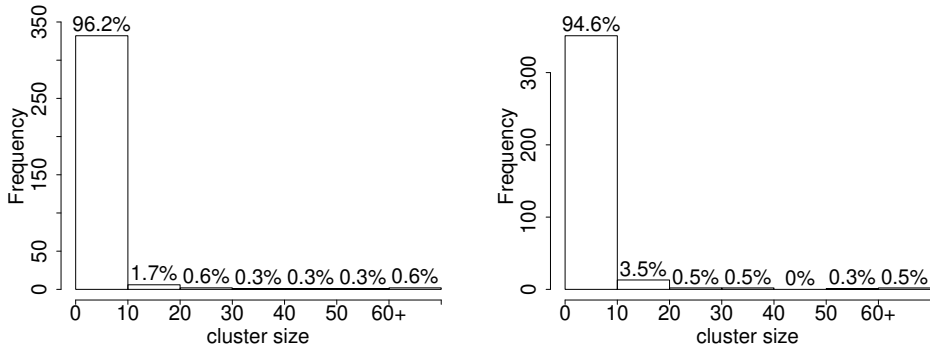


Figure 6. Distribution of the cluster size for the NN-catalog (left) and the SD catalog (right).

Table 2. Selection of large earthquake clusters identified by both declustering methods. The table lists: date and magnitude of the largest event in the cluster; cluster size based on the NN-method and the SD-method; number of events identified by both methods.

| <i>largest event</i> | <i>cluster size</i> | | matched events | <i>largest event</i> | <i>cluster size</i> | | matched events |
|------------------------|---------------------|-----|----------------|-----------------------|---------------------|----|----------------|
| | NN | SD | | | NN | SD | |
| 12 April 1998 M5.6 | 720 | 757 | 682 | 20 April 1994 M3.7 | 21 | 27 | 21 |
| 12 July 2004 M5.1 | 201 | 238 | 196 | 14 February 2002 M4.9 | 19 | 14 | 14 |
| 13 April 1996 M4.3 | 52 | 52 | 48 | 5 October 1991 M3.8 | 18 | 19 | 18 |
| 16 September 1977 M5.2 | 41 | 38 | 36 | 12 February 2013 M3.8 | 15 | 12 | 11 |
| 1 February 1988 M4.1 | 34 | 39 | 34 | 25 February 2018 M3.9 | 15 | 15 | 15 |
| 18 April 1979 M4.8 | 28 | 12 | 12 | 29 August 2015 M4.3 | 5 | 14 | 5 |

290 say that they are matched clusters. In our application we found exactly 241 pairs of matched
 291 clusters.

292 Table 2 lists some significant clusters, reporting their cluster size according to NN-
 293 method and SD-method, as well as the number of events associated by both methods,
 294 i.e. the matched events. We notice that, in general, the number of matching events be-
 295 tween NN-clusters and SD-clusters is sizable compared to the total cluster size; there-
 296 fore we can state that the two declustering methods roughly identify the same earthquake
 297 clusters. However, this comparison neglects the links between the events, which are es-
 298 tablished by each declustering method. In section 5 we deepen the comparison between
 299 NN-clusters and SD-clusters by analyzing also their internal structure.

300 5 Topological Structure of Earthquake Clusters

301 Connections between events of a cluster, as established by the considered declus-
 302 tering methods, allow us to represent the cluster as a network graph. In this section we
 303 focus on some centrality measures developed in network theory, which should quantita-
 304 tively express the way earthquakes get organized within clusters.

305 5.1 Tree graph representation of clusters

306 By construction, the identified clusters are organized in rooted time-oriented tree
 307 graphs, where each tree root represents the triggering event and the other nodes are the
 308 triggered secondary events. For example, Fig. 7 illustrates the tree graph representation
 309 of the earthquake cluster occurred in 1988, according to NN-algorithm (left) and SD-algorithm
 310 (right). Nodes are joined by edges, which represent the connections between pairs of events.
 311 Each node (event), other than the root, is directly connected to its only parent (which
 312 triggers the event); in other words, that node is a direct descendant of its parent. The
 313 nodes along the path between the root and a node v are named ancestors of node v . The
 314 descendants of node v are those nodes of which v is an ancestor.

315 It is worth noting that the triggering earthquake of the sequence (tree root) is not
 316 necessarily the strongest event of the cluster. Let us consider, for instance, the 1988 clus-
 317 ter (Fig. 7): both declustering methods recognised that the 1 February 1988 11:12:41.28
 318 earthquake, with magnitude M3.0, is the triggering earthquake of the sequence; there-
 319 fore, this event turns out to be an ancestor of the largest event within the cluster, an earth-
 320 quake with magnitude M4.1 that occurred on 1 February 1988 14:21:38.29.

321 As for 1988 cluster, there is little difference between NN-cluster and SD-cluster in
 322 terms of cluster size, tree graphs, and spatio-temporal distribution of the cluster events

323 (Tab. 2 and Fig. 7). But this is not always the case. Indeed we noticed that NN-method
 324 is prone to cluster some events relatively distant in space and, conversely, SD-method
 325 tends to cluster events close in space, but quite far in time, as for the clusters occurred
 326 in 1996 and 1998, respectively (e.g. Figs. 8-9). Moreover, SD-method may provide a more
 327 complex structure for clusters, reflecting the multilevel triggering property of the ETAS
 328 model (Fig. 9).

329 5.2 Some centrality measures

330 We have chosen some tools from network theory in order to study the structural
 331 properties of clusters through their network representations (tree graphs).

332 We focus hereafter on the concept of *centrality measure*, which is strictly related
 333 to the topology (structural properties) of the network (Freeman, 1978). A centrality value
 334 is attributed to each node according to its importance (centrality) within the network.
 335 Since “importance” has a relative meaning and appropriate interpretation with respect
 336 to circumstances, several centrality measures have been proposed in the literature (Wasserman
 337 and Faust (1994), Freeman (1978), Bonacich (1987), Bonacich and Lloyd (2001), Borgatti
 338 (2005), and references therein). A brief overview of two centrality measures we consid-
 339 ered as relevant for our analysis, is provided hereinafter.

340 *Outdegree centrality.* The simplest centrality measures are based on the degree, in-
 341 degree, and outdegree of a node v , which are respectively defined as the number of edges
 342 (links) that are connected to v , the number of incoming edges to v , and the number of
 343 outgoing edges from v . We notice that, by construction, each event of a declustered cat-
 344 alog has indegree equal to 0 or 1 (corresponding to background events or secondary events,
 345 respectively), and we expect that high outdegrees are especially associated with main-
 346 shocks within a cluster. Therefore outdegree turns out to be more suitable than inde-
 347 gree in our application. Let $\delta(v)$ be the outdegree of node v in tree T ,

$$348 \quad \delta(v|T) = \text{number of edges in tree } T \text{ that go down from } v. \quad (5)$$

349 Since the outdegree of a node is at most $\#T-1$, where $\#T$ is the total number of nodes
 350 in T , the outdegree centrality of v is defined as the proportion of direct offsprings from
 351 v in the entire tree T :

$$352 \quad c_\delta(v|T) = \frac{\delta(v|T)}{\#T - 1} \quad , \quad (6)$$

353 so as to obtain a measure independent on network size. Outdegree centrality ranges in
 354 $[0, 1]$, where high degree values denote the most important nodes, to which most of the
 355 events are connected.

356 *Closeness centrality.* The most important node according to closeness centrality
 357 has minimum distance from every other nodes. Closeness centrality of a node v is de-
 358 fined as

$$359 \quad c_c(v|T) = \frac{\#T - 1}{\sum_{w \in T} d(v, w)} \quad , \quad (7)$$

360 where $d(v, w)$ is the shortest distance in T from v to w (i.e., the number of edges in the
 361 shortest path from v to w); the numerator $\#T-1$ is the minimum value that the sum
 362 in the denominator can take. If there is no path from v to w (e.g. from a node to the
 363 root), then $d(v, w)$ is set equal to the total number of nodes in T . Closeness centrality
 364 ranges in $[0, 1]$ and, in analogy with outdegree centrality, high degree values denote the
 365 most important nodes.

366 Finally, a global index, named *centralization*, is introduced in order to summarize
 367 the centrality measures of all the nodes in the network: Centralization quantifies the dif-
 368 ferences between the centrality of the most central node v^* and that of all other nodes.

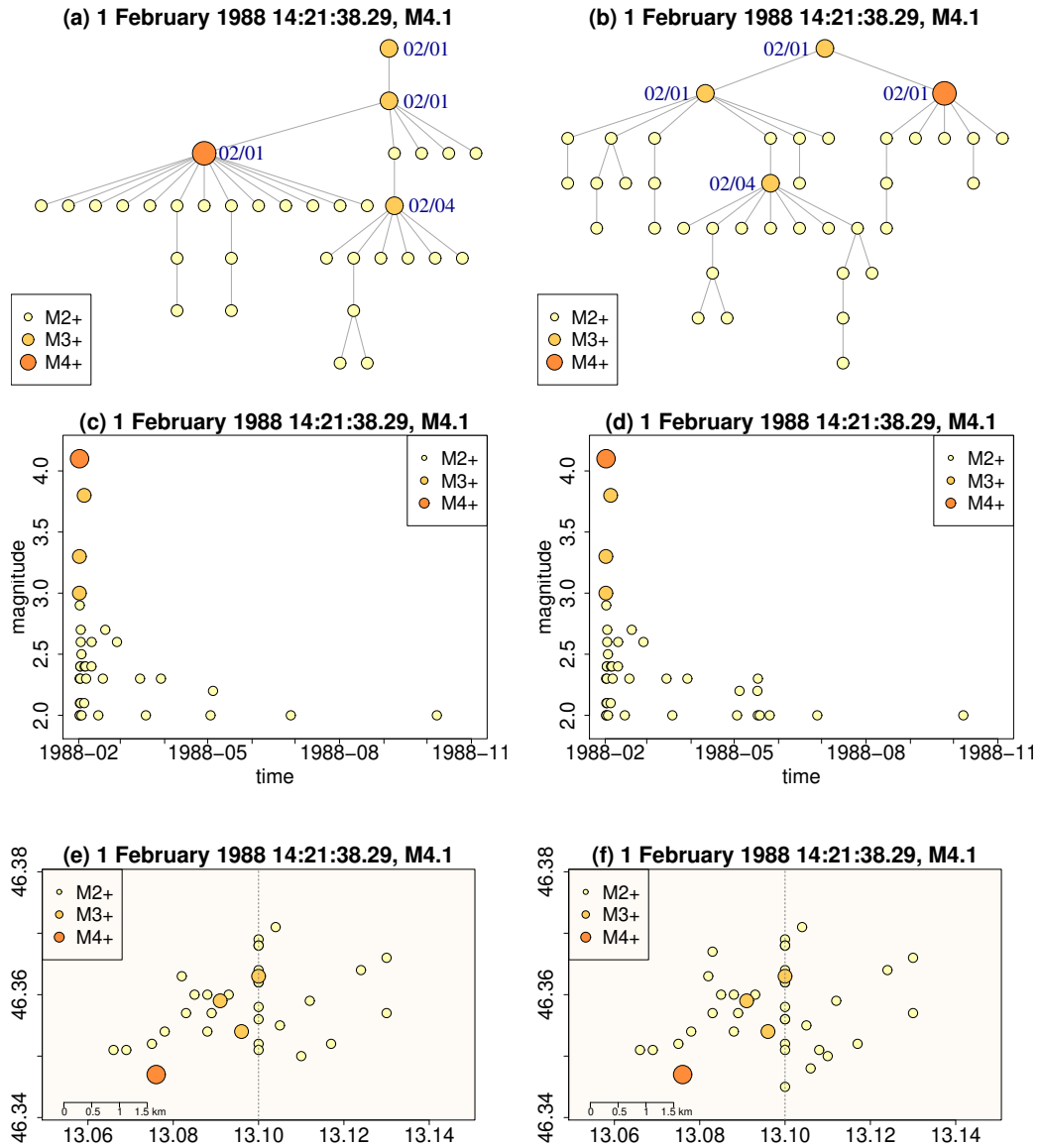


Figure 7. NN-cluster (left) and SD-cluster (right) of the seismic sequence occurred in 1988: (a-b) tree graph representation, (c-d) magnitude versus occurrence times, (e-f) map of the epicenters. Date and magnitude of the largest event is also reported.

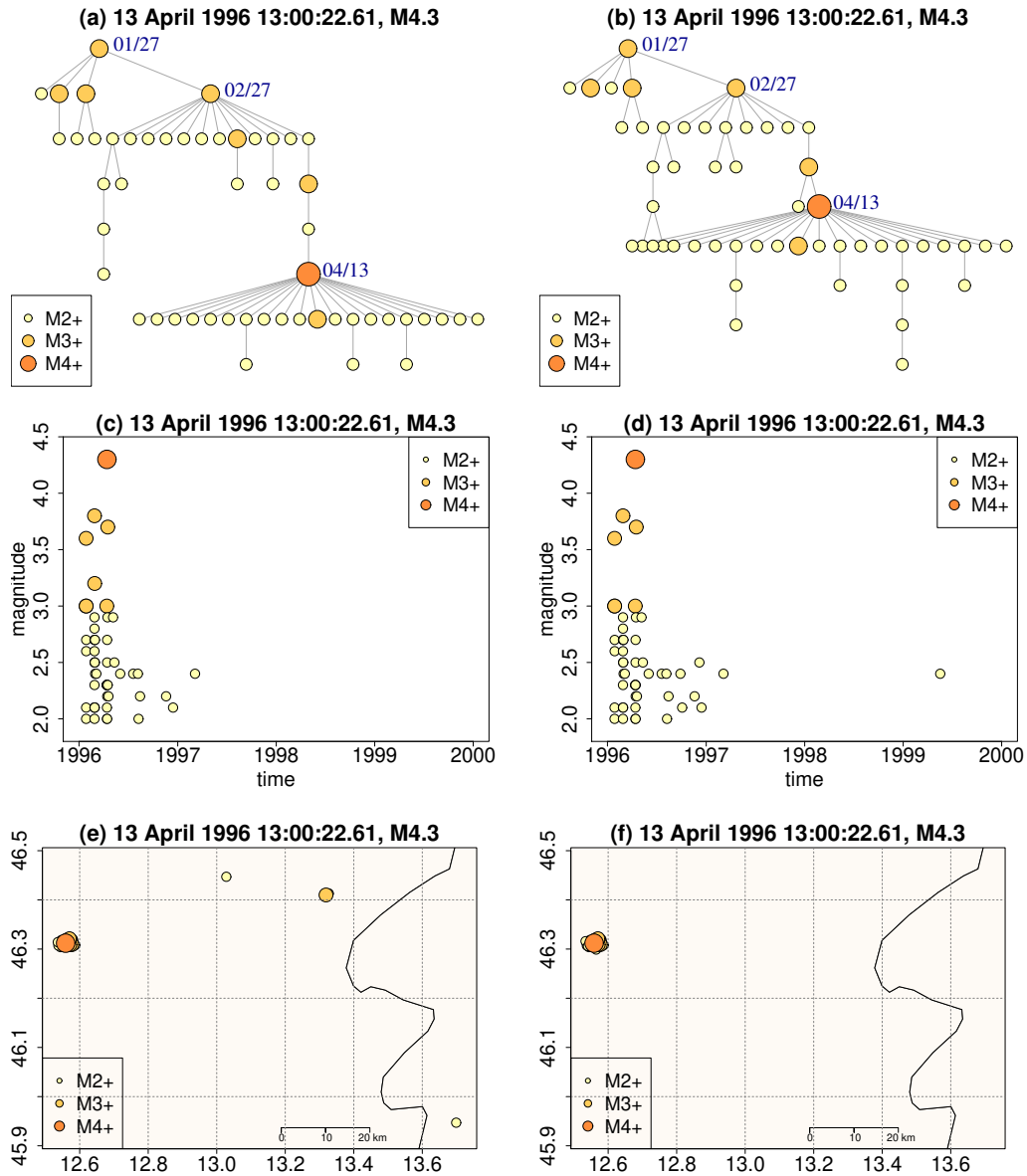


Figure 8. NN-cluster (left) and SD-cluster (right) of the seismic sequence occurred in 1996: (a-b) tree graph representation, (c-d) magnitude versus occurrence times, (e-f) map of the epicenters. Date and magnitude of the largest event is also reported.

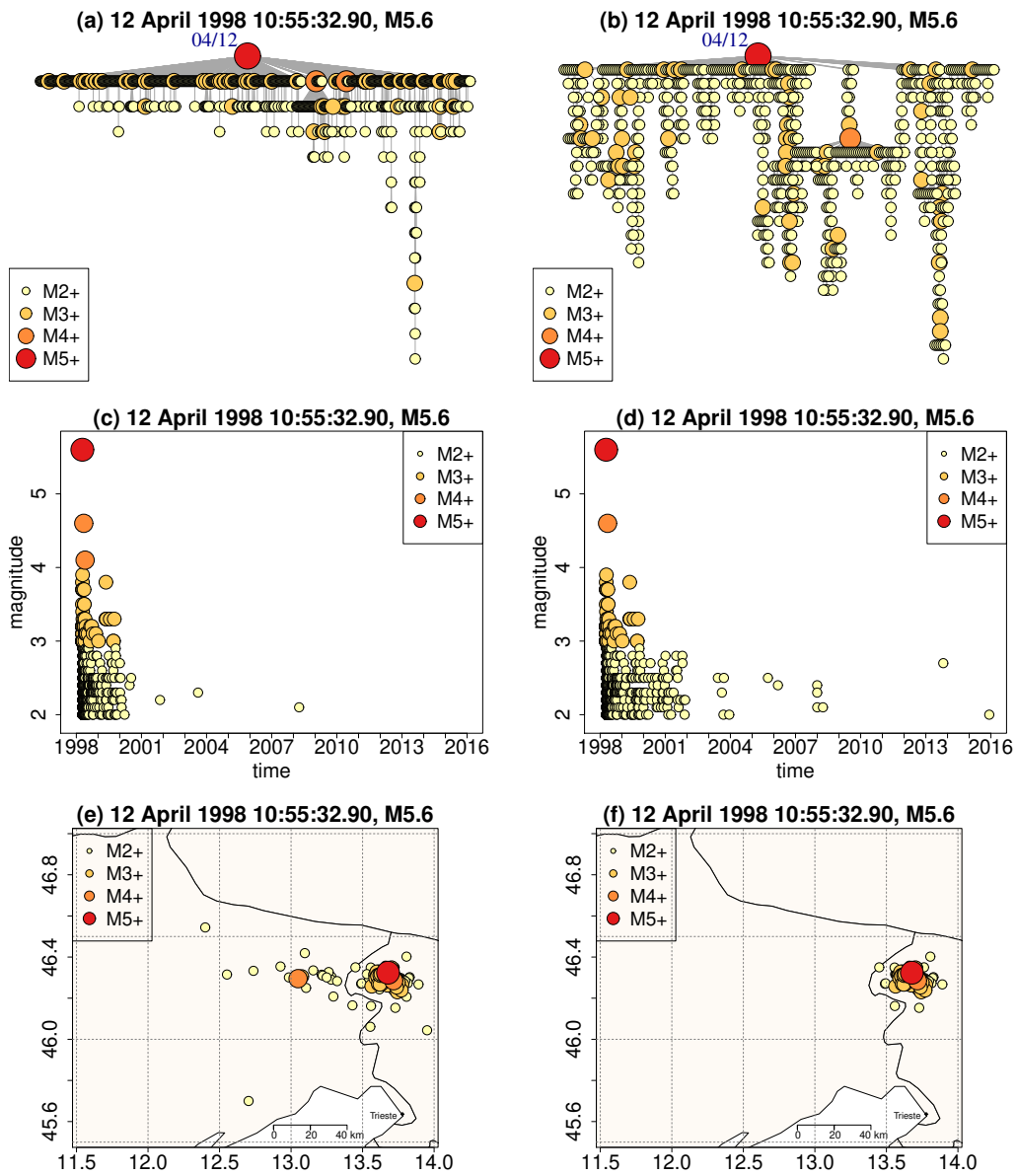


Figure 9. NN-cluster (left) and SD-cluster (right) of the seismic sequence occurred in 1998: (a-b) tree graph representation, (c-d) magnitude versus occurrence times, (e-f) map of the epicenters. Date and magnitude of the largest event is also reported.

369 The following formulas define the centralization based on outdegree centrality and close-
 370 ness centrality:

$$371 \quad C_\delta(T) = \frac{\sum_v c_\delta(v^*|T) - c_\delta(v|T)}{\#T - 1} \quad \text{outdegree centralization,} \quad (8)$$

$$372 \quad C_c(T) = \frac{\sum_v c_c(v^*|T) - c_c(v|T)}{\#T - 1} \quad \text{closeness centralization.} \quad (9)$$

374 Centralization also ranges in $[0, 1]$ and high centralization indicates the tendency of a
 375 single node (i.e. an earthquake) to be more central than other nodes in the network (i.e.
 376 in the cluster). Both centrality measures and centralization are normalized on $[0, 1]$ and
 377 thus independent on the cluster size; this makes the topological comparison among tree
 378 graphs easier, compared to the use of other indices (e.g., average node depth and aver-
 379 age leaf depth proposed by Zaliapin and Ben-Zion (2013)), especially for clusters with
 380 very different numbers of nodes.

381 Tab. 3 lists the centralization values of matched clusters with large cluster size. Fig. 10
 382 compares all the matched clusters that have at least 5 events, in terms of both C_δ and
 383 C_c . Fig. 11 shows the spatial distribution of the epicentres of the representative events
 384 for all the matched NN-clusters and the SD-clusters. Overall, it emerges that central-
 385 ization values of the NN-clusters are comparable to or higher than those of the SD-clusters.
 386 Thus, both centralizations C_δ and C_c are proved to be effective indices for expressing
 387 what has been observed in Figs. 7-9: whenever a NN-cluster exhibits similar or even sim-
 388 pler structural complexity than its matched SD-cluster, its centralization value is sim-
 389 ilar to or greater than that of its matched SD-cluster.

390 We also verified that C_δ and C_c have a strong positive correlation to each other (0.87
 391 for NN-clusters and 0.86 for SD-clusters). Their correlations to the magnitudes of the
 392 representative events are moderate (0.60 and 0.46 for NN-clusters, and 0.42 and 0.26 for
 393 SD-clusters, respectively) and also their correlations with clusters size are close to zero
 394 (between -0.2 and 0.2). This suggests that the complexity of clusters structure does not
 395 depend simply on magnitude and related clusters size.

396 The spatial distribution of centralization values obtained for NN- and SD-clusters
 397 (Fig. 11) highlights the basic difference between the two approaches, namely the com-
 398 paratively higher complexity of SD-clusters structure, which reflects the multilevel trig-
 399 gering property of this approach; in the color scale dark colors correspond to low val-
 400 ues of centralization, which are associated with swarm-like sequences, whereas light col-
 401 ors correspond to burst-like sequences. This is particularly evident for the largest earth-
 402 quakes (events with $M \geq 5$ in Table 2), which are represented by stars in the maps. These
 403 events are associated to rather simple clusters by NN (i.e. high centrality values, close
 404 to 1), whereas they correspond to complex clusters in SD (i.e. low centrality values, close
 405 to 0); this effect is less evident for the 1977 earthquake, possibly because the event oc-
 406 curred at the beginning of the considered data set. In addition, while the spatial distri-
 407 bution of centralization values from NN-clusters does not contradict the spatial pattern
 408 identified by Peresan and Gentili (2018), in both maps from SD-clusters, the complex
 409 swarm-like sequences appear scattered all over the study area.

410 6 Conclusions

411 In this study, we compared the performances of the NN and SD algorithms in clas-
 412 sifying events from an earthquake catalogue into clusters and background seismicity. Both
 413 methods provide data-driven identifications of earthquake clusters and permit to disclose
 414 possible complex features in their internal structure. The two declustering algorithms
 415 have been applied to the seismicity data of Northeastern Italy, whose completeness and
 416 scaling parameters were already analysed in some detail by Peresan and Gentili (2018).

Table 3. Centralization scores based on outdegree centrality (C_δ) and on closeness centrality (C_c) for the selection of matched large clusters listed in Table 2. The clusters including earthquakes with $M \geq 5$ are marked by numbers as in Fig. 10.

| <i>largest event</i> | C_δ | | C_c | |
|---------------------------------------|-------------------|-------------------|-------------------|-------------------|
| | <i>NN-cluster</i> | <i>SD-cluster</i> | <i>NN-cluster</i> | <i>SD-cluster</i> |
| ⁽¹⁾ 12 April 1998 M5.6 | 0.6490 | 0.1868 | 0.6307 | 0.1601 |
| ⁽²⁾ 12 July 2004 M5.1 | 0.8191 | 0.4576 | 0.7832 | 0.1431 |
| 13 April 1996 M4.3 | 0.3802 | 0.3602 | 0.2274 | 0.2335 |
| ⁽⁴⁾ 16 September 1977 M5.2 | 0.8462 | 0.5836 | 0.8472 | 0.6763 |
| 1 February 1988 M4.1 | 0.3756 | 0.1627 | 0.2632 | 0.2754 |
| 18 April 1979 M4.8 | 0.4623 | 0.5041 | 0.4798 | 0.5013 |
| 20 April 1994 M3.7 | 0.5275 | 0.4808 | 0.1898 | 0.2162 |
| 14 February 2002 M4.9 | 0.8827 | 0.9172 | 0.4466 | 0.4476 |
| 5 October 1991 M3.8 | 0.5640 | 0.2377 | 0.3855 | 0.2052 |
| 12 February 2013 M3.8 | 0.1200 | 0.1074 | 0.1798 | 0.1063 |
| 25 February 2018 M3.9 | 0.4643 | 0.3878 | 0.3737 | 0.3351 |
| 29 August 2015 M4.3 | 1.0000 | 0.6686 | 1.0000 | 0.6985 |

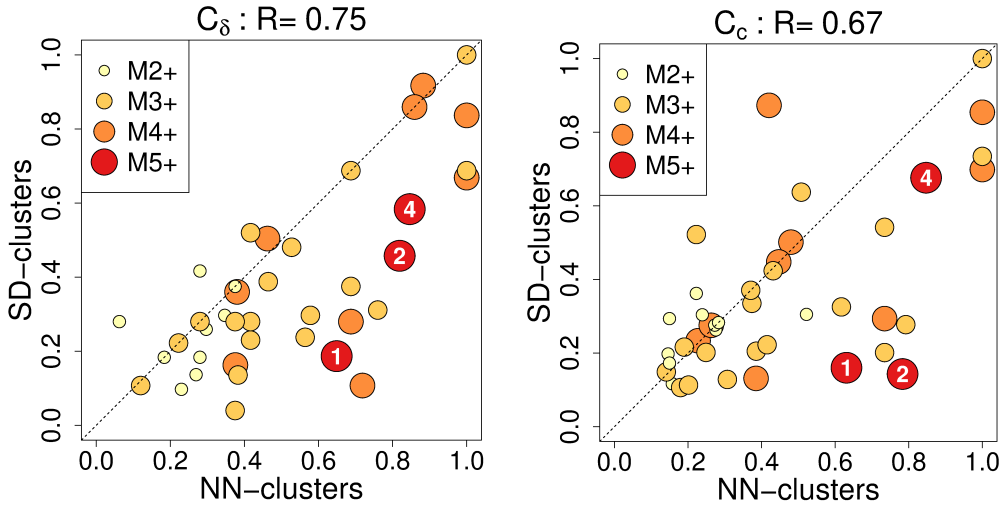


Figure 10. Comparison of the matched clusters that have at least 5 events, in terms of outdegree centralization (left) and closeness centralization (right); correlation values are also reported. The colors and sizes of the dots refer to the magnitude level of the largest event in the clusters. Numbered symbols refer to the events listed in Tab. 3.

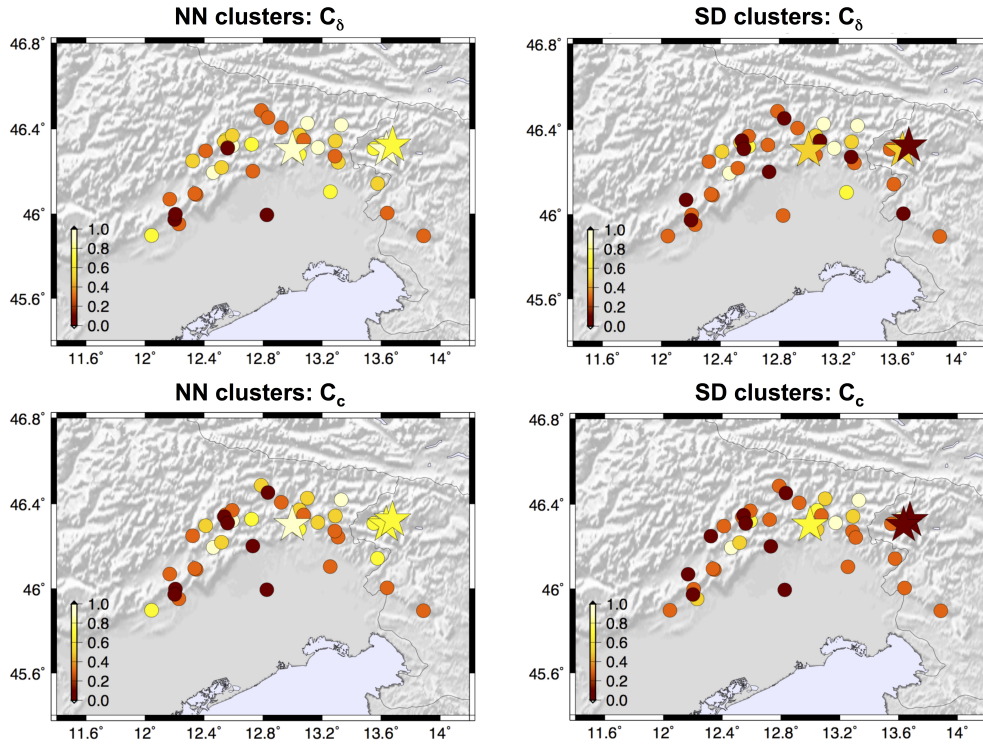


Figure 11. Spatial distribution of the epicentres of the representative events (the largest events within each of the NN-clusters (left) and the SD-clusters (right)) for the clusters that have at least 5 events. Each epicentre is associated with the outdegree centralization (top) or the closeness centralization (bottom) of its cluster. The matched clusters are denoted by circles and the events with $M \geq 5$ are highlighted by stars.

417 The global features of the resulting background seismicity and earthquake clusters
 418 turn out well consistent, though the partitions are slightly different. Specifically, the statis-
 419 tics of clusters, singles and fore/aftershocks are quite comparable (Tab. 1). Both NN and
 420 SD results consistently show that background seismicity is composed by a large propor-
 421 tion of single events (about 45-50%) and by a limited number of clustered events (8-9%).
 422 However the events forming the background may be different (especially in presence of
 423 foreshocks), due to the different definitions used by the two methods: NN assigns to back-
 424 ground the largest earthquake from each cluster, whereas SD the first independent earth-
 425 quake in the cluster.

426 Since the two methods also allow to outline the internal structure of clusters, an
 427 in-depth comparison was carried out both for selected clusters (Figs. 7, 8, 9) and for all
 428 matching clusters identified by NN and SD (Figs. 10, 11). The concepts of outdegree cen-
 429 trality and closeness centrality have been introduced from network theory to quantita-
 430 tively compare the characteristics of the declustering outputs, by regarding earthquake
 431 clusters as tree graphs. The proposed centrality measures, C_δ and C_c , are especially ad-
 432 vantageous when clusters with different and large sizes are compared; in these cases, the
 433 tree graph representation of the cluster might be very unclear due to the large number
 434 of nodes, while centralization indices are still able to capture some key properties of the
 435 hierarchical complexity of the cluster and to rank earthquakes within the cluster accord-
 436 ing to their importance/centrality. These quantitative measures are shown to be able to
 437 characterize the internal structure of the clusters in a robust and consistent way. Accord-
 438 ingly, we found that NN-clusters usually display simpler internal structures than SD-clusters
 439 and that the corresponding centralization values of NN-clusters are higher than those
 440 of SD-clusters.

441 Given the outcomes of this in-depth comparative analysis of NN and SD methods,
 442 there are still some open issues that need to be addressed and will be matter for future
 443 research. The main outcome of this study consists in the identification of the basic sim-
 444 ilarities and differences between the NN and SD methods, both in their theoretical for-
 445 mulation and operational results. From a methodological point of view, we believe the
 446 use of centrality measures and other tools borrowed from network theory may open new
 447 possibilities in the study of earthquake sequences and their evolution. Another issue is
 448 to verify generality of above conclusions, that is to assess to what extent they depend
 449 on the considered catalog and study area by performing the same analysis in different
 450 regions. Finally, there is the problem of investigating how these declustering algorithms
 451 influence the forecasting performance in short-term and long-term earthquake hazard
 452 assessment.

453 Acknowledgments

454 This work is supported by National grant MIUR, PRIN-2015 program, Prot. 20157PRZC4: Complex
 455 space-time modeling and functional analysis for probabilistic forecast of seismic events.
 456 J. Zhuang is also partially supported by the JSPS Grant-in-aid 19H04073. We also ac-
 457 knowledge financial support from Civil Defence of the Friuli Venezia Giulia Region. Graph
 458 visualization is realized by the R package *igraph* (Csardi & Nepusz, 2006). Earthquake
 459 data used in this study are published as yearly and monthly bulletins by the National
 460 Institute of Oceanography and Experimental Geophysics (OGS) and are publicly avail-
 461 able via the OGS website (<http://www.crs.inogs.it/bollettino/RSFVG/>).

462 References

- 463 Baiesi, M., & Paczuski, M. (2004). Scale-free networks of earthquakes and after-
 464 shocks. *Physical Review E*, *69*, 066106. doi: 10.1103/PhysRevE.69.066106
 465 Bonacich, P. (1987). Power and centrality: A family of measures. *American Journal*
 466 *of Sociology*, *92*(5), 1170-1182. doi: 10.1086/228631

- 467 Bonacich, P., & Lloyd, P. (2001). Eigenvector-like measures of centrality for
 468 asymmetric relations. *Social Networks*, *23*(3), 191 - 201. doi: 10.1016/
 469 S0378-8733(01)00038-7
- 470 Borgatti, S. P. (2005). Centrality and network flow. *Social Networks*, *27*(1), 55 - 71.
 471 doi: 10.1016/j.socnet.2004.11.008
- 472 Csardi, G., & Nepusz, T. (2006). The igraph software package for complex network
 473 research. *InterJournal, Complex Systems*, 1695. (<http://igraph.org>)
- 474 Davoudi, N., Tavakoli, H. R., Zare, M., & Jalilian, A. (2018). Declustering
 475 of Iran earthquake catalog (1983-2017) using the epidemic-type after-
 476 shock sequence (ETAS) model. *Acta Geophysica*, *66*(6), 1359-1373. doi:
 477 10.1007/s11600-018-0211-5
- 478 Freeman, L. C. (1978). Centrality in social networks. conceptual clarification. *Social*
 479 *Networks*, *1*(3), 215–239. doi: 10.1016/0378-8733(78)90021-7
- 480 Gardner, J. K., & Knopoff, L. (1974). Is the sequence of earthquakes in southern
 481 California, with aftershocks removed, Poissonian? *Bulletin of the Seismological*
 482 *Society of America*, *64*(5), 1363-1367.
- 483 Guo, Y., Zhuang, J., Hirata, N., & Zhou, S. (2017). Heterogeneity of direct af-
 484 tershock productivity of the main shock rupture. *Journal of Geophysical Re-*
 485 *search: Solid Earth*, *122*(7), 5288–5305. doi: 10.1002/2017JB014064
- 486 Guo, Y., Zhuang, J., & Zhou, S. (2015). An improved space-time ETAS model for
 487 inverting the rupture geometry from seismicity triggering. *Journal of Geophys-*
 488 *ical Research: Solid Earth*, *120*(5), 3309–3323. doi: 10.1002/2015JB011979
- 489 Nandan, S., Ouillon, G., Sornette, D., & Wiemer, S. (2019). Forecasting the rates of
 490 future aftershocks of all generations is essential to develop better earth-
 491 quake forecast models. *Journal of Geophysical Research: Solid Earth*, *124*(8),
 492 8404-8425. doi: 10.1029/2018JB016668
- 493 Nekrasova, A., Kossobokov, V., Peresan, A., Aoudia, A., & Panza, G. F. (2011). A
 494 multiscale application of the unified scaling law for earthquakes in the central
 495 mediterranean area and alpine region. *Pure and Applied Geophysics*, *168*(1),
 496 297–327. doi: 10.1007/s00024-010-0163-4
- 497 Ogata, Y. (1998). Space-time point-process models for earthquake occurrences. *An-*
 498 *nals of the Institute of Statistical Mathematics*, *50*(2), 379–402. doi: 10.1023/
 499 A:1003403601725
- 500 Peresan, A., & Gentili, S. (2018). Seismic clusters analysis in Northeastern Italy by
 501 the nearest-neighbor approach. *Physics of the Earth and Planetary Interiors*,
 502 *274*, 87 - 104. doi: 10.1016/j.pepi.2017.11.007
- 503 Reasenber, P. (1985). Second-moment of central California seismicity, 1969–1982.
 504 *Journal of Geophysical Research*, *90*(B7), 5479–5495.
- 505 Rotondi, R. (2010). Bayesian nonparametric inference for earthquake recurrence
 506 time distributions in different tectonic regimes. *Journal of Geophysical Re-*
 507 *search: Solid Earth*, *115*(B1), 1–25. doi: 10.1029/2008JB006272
- 508 Rotondi, R., & Varini, E. (2019). Failure models driven by a self-correcting point
 509 process in earthquake occurrence modeling. *Stochastic Environmental Research*
 510 *and Risk Assessment*, *33*(3), 709–724. doi: 10.1007/s00477-019-01663-5
- 511 Rovida, A., Locati, M., Camassi, R., Lolli, B., & Gasperini, P. (2014). *Italian*
 512 *Parametric Earthquake Catalogue (CPTI15), version 2.0. Istituto Nazionale di*
 513 *Geofisica e Vulcanologia (INGV)*. (<https://doi.org/10.13127/CPTI/CPTI15.2>)
- 514 Slejko, D., Neri, G., Orozova, I., Renner, G., & Wyss, M. (1999). Stress field in friuli
 515 (ne italy) from fault plane solutions of activity following the 1976 main shock.
 516 *Bulletin Seismological Society of America*, *89*(4), 1037–1052.
- 517 Talbi, A., Nanjo, K., Satake, K., Zhuang, J., & Hamdache, M. (2013). Comparison
 518 of seismicity declustering methods using a probabilistic measure of clustering.
 519 *Journal of Seismology*, *17*(3), 1041–1061. doi: 10.1007/s10950-013-9371-6
- 520 van Stiphout, T., Zhuang, J., & Marsan, D. (2012). Seismicity declustering. *Com-*
 521 *munity Online Resource for Statistical Seismicity Analysis*, 1–25. (Available at

- 522 <http://www.corssa.org> doi: 10.5078/corssa-52382934
- 523 Vere-Jones, D. (1978). Earthquake prediction - A statistician's view. *Journal of*
 524 *Physics of the Earth*, 26(2), 129-146. doi: 10.4294/jpe1952.26.129
- 525 Wang, Q., Jackson, D. D., & Zhuang, J. (2010). Are spontaneous earthquakes sta-
 526 tionary in California? *Journal of Geophysical Research: Solid Earth*, 115(B8),
 527 1–12. doi: 10.1029/2009JB007031
- 528 Wasserman, S., & Faust, K. (1994). *Social network analysis: Methods and applica-*
 529 *tions*. Cambridge University Press. doi: 10.1017/CBO9780511815478
- 530 Zaliapin, I., & Ben-Zion, Y. (2013). Earthquake clusters in southern California II:
 531 Classification and relation to physical properties of the crust. *Journal of Geo-*
 532 *physical Research: Solid Earth*, 118(6), 2865-2877. doi: 10.1002/jgrb.50178
- 533 Zaliapin, I., & Ben-Zion, Y. (2016). A global classification and characterization of
 534 earthquake clusters. *Geophysical Journal International*, 207(1), 608-634. doi:
 535 10.1093/gji/ggw300
- 536 Zaliapin, I., Gabrielov, A., Keilis-Borok, V., & Wong, H. (2008, Jun). Cluster-
 537 ing analysis of seismicity and aftershock identification. *Phys. Rev. Lett.*, 101,
 538 018501. doi: 10.1103/PhysRevLett.101.018501
- 539 Zhang, Q., & Shearer, P. M. (2016). A new method to identify earthquake swarms
 540 applied to seismicity near the San Jacinto Fault, California. *Geophysical Jour-*
 541 *nal International*, 205(2), 995-1005. doi: 10.1093/gji/ggw073
- 542 Zhuang, J. (2006). Second-order residual analysis of spatiotemporal point processes
 543 and applications in model evaluation. *Journal of the Royal Statistical Society:*
 544 *Series B (Statistical Methodology)*, 68(4), 635–653. doi: 10.1111/j.1467-9868
 545 .2006.00559.x
- 546 Zhuang, J., Chang, C.-P., Ogata, Y., & Chen, Y.-I. (2005). A study on the back-
 547 ground and clustering seismicity in the Taiwan region by using point process
 548 models. *Journal of Geophysical Research: Solid Earth*, 110(B5), 1–12. doi:
 549 10.1029/2004JB003157
- 550 Zhuang, J., Ogata, Y., & Vere-Jones, D. (2002). Stochastic declustering of space-
 551 time earthquake occurrences. *Journal of the American Statistical Association*,
 552 97(3), 369–380.
- 553 Zhuang, J., Ogata, Y., & Vere-Jones, D. (2004). Analyzing earthquake clustering
 554 features by using stochastic reconstruction. *Journal of Geophysical Research:*
 555 *Solid Earth*, 109(3), B05301. doi: 10.1029/2003JB002879